Matter and Radiation at Extremes

RESEARCH ARTICLE

pubs.aip.org/aip/mre

Nonstationary laser-supported ionization wave in layer of porous substance with subcritical density

Cite as: Matter Radiat. Extremes 9, 016601 (2024); doi: 10.1063/5.0157904
Submitted: 12 May 2023 • Accepted: 4 September 2023 •
Published Online: 14 November 2023

S. Yu Gus'kov and R. A. Yakhin[a)]

AFFILIATIONS

P.N. Lebedev Physical Institute of Russian Academy of Sciences, Leninskii Prospect 53, Moscow 119991, Russia

[a)]Author to whom correspondence should be addressed: yakhin.rafael@gmail.com

ABSTRACT

A time-dependent analytical solution is found for the velocity of a plane ionization wave generated under nanosecond laser pulse action on the surface of a flat layer of low-Z porous substance with density less than the critical density of the produced plasma. With corrections for the two-dimensional nature of the problem when a laser beam of finite radius interacts with a flat target, this solution is in quantitative agreement with measurements of ionization wave velocity in various experiments. The solution compared with experimental data covering wide ranges of performance conditions, namely, (3–8) × 10^{14} W cm^{-2} for laser pulse intensity, 0.3–3 ns for pulse duration, 0.35–0.53 μm for laser wavelength, 100–1000 μm for laser beam radius, 380–950 μm for layer thickness, 4.5–12 mg cm^{-3} for average density of porous substance, and 1–25 μm for average pore size. The parameters of the laser beam that ensure the generation of a plane ionization wave in a layer of subcritical porous matter are determined for the problem statements and are found to meet the requirements of practical applications.

I. INTRODUCTION

Plasmas produced by the action of lasers on low-density porous substances are of great interest for research into fundamental plasma phenomena, as well as with regard to possible practical applications. Here, the porous substances should have density close to the critical plasma density corresponding to short-wavelength laser radiation, such as the first three harmonics of an Nd laser. Such media with density in the approximate range of 1–10 mg cm^{-3} have a very high porosity, exceeding 0.95. This high porosity, where voids occupy more than 95% of the substance's volume, determines the distinctive features of laser interaction with the substance and the properties of the produced plasma. These features are associated with the fact that the plasma creation is accompanied by a leveling of density (homogenization). Homogenization occurs as a result of the ion–ion Coulomb scattering when plasma flowing from the heated pore walls collides inside the pores. The homogenization rate depends on the parameters of the porous structure and the power of the heating source power. In a high-porosity substance, multiple collisions of plasma flows inside a single pore are needed for density equalization.[1] For this reason, the laser-produced plasma exists in a state of partial homogenization for a relatively long period of time, comparable to the duration of the heating laser pulse duration.[1,2] Even in a porous substance with supercritical average density, laser light is absorbed in the volume of partially homogenized plasma with geometric transparency depth, where it can penetrate through micro-sized regions with subcritical density. This explains not only the high fraction of nanosecond laser pulse energy absorbed in low-density porous media, but also the weak dependence of its value on the laser wavelength. In experiments,[3–8] it was found that up to 80%–90% of the radiation energy of the first three Nd-laser harmonics was absorbed in porous substances with both subcritical and supercritical densities. The peculiarities of the thermodynamic and transport properties of a partly homogenized plasma are related to the fact that some fraction of the internal energy is contained in the energy of turbulent motion of plasma flows. This is the reason for the delayed formation of hydrodynamic motion and suppression of electron heat conductivity during the homogenization period.[1,2]

Low-Z porous media such as porous plastics (CH_n) and cellulose triacetate (TAC) with density from several to several tens of mg cm^{-3} have a micro-sized structure consisting of interconnected

open or closed pores. The pore configuration is determined by solid elements in the form of flat membranes, extended filaments, or a mixed membrane–filament structure. The structural parameters of these substances can vary over a wide range.[9] The average pore size can range from several tens of micrometers to submicrometer values, with the respective thicknesses of the solid elements (membranes or filaments) also being on the micrometer and submicrometer scales. Such media can withstand the addition of nano-sized clusters of heavy chemical elements such as gold or copper with mass fractions up to 20%–30%.[9]

In high-energy-density physics, interest in laser-produced plasmas of low-density porous media is associated mainly with the research into laser thermonuclear fusion (inertial confinement fusion, ICF) and equations of state (EOS) of matter. In the first case, it has been proposed to use porous substances as absorbers of laser pulse radiation, thus providing effective smoothing of inhomogeneities in target heating.[10–12] In the second case, such absorbers can provide the generation of shock waves with controllable spatial–temporal propagation characteristics.[13–16] An important property of these porous substances in this context is that, unlike gaseous media, they does not impose special technical requirements when used in experiments.

The formation of laser-produced plasmas of porous substances with supercritical density occurs, ultimately, under conditions of shock wave generation. By contrast, in substances with subcritical density, the absorbed laser energy transfer is provided by an ionization wave expanding the region where laser radiation is absorbed. This paper is devoted to the development of a theory of just such a phenomenon of a laser-supported ionization wave in a porous substance with subcritical density. The first model of a laser-supported ionization wave in a porous substance with account taken of the homogenization process, was proposed in Ref. 17, where a time-integrated correction was calculated for the solution given in Ref. 18 for the velocity of the ionization wave in a continuous substance with subcritical density. The effect of ionization wave deceleration in a porous substance in comparison with the case of a continuous substance was confirmed in various experiments.[3,4,19–25] The model in Ref. 17 has been used in one or another form for numerical simulations of nanosecond laser pulse interaction with porous substances.[8,16,19,26–31]

In the present paper, an analytical solution is obtained for the velocity of a nonstationary laser-supported ionization wave and for the thermodynamic characteristics of the produced plasma, considering their dependence on the parameters of the porous substance and the heating laser pulse. Section II presents the solution for a plane ionization wave. The one-dimensional (1D) model is a key result of this paper, since it is plane waves that are of interest for the above noted applications. Section III is devoted to testing of the 1D solution on the basis of experimental results. To compare the results of the theory with those of experiments, all of which were performed by irradiating a flat target with a laser beam of a finite radius, the 1D solution is supplemented with corrections describing the influence of two-dimensional (2D) effects. Finally, in Sec. IV, the parameters of the laser beam that ensure the generation of a plane ionization wave in a layer of porous material of subcritical density are determined for wide ranges of laser and target parameters.

II. ANALYTICAL SOLUTION FOR NONSTATIONARY LASER-SUPPORTED IONIZATION WAVE IN POROUS LAYER OF FINITE THICKNESS

The propagation is considered of a plane ionization wave induced by a laser pulse (with a time-constant intensity) in a layer of porous substance with average density smaller than the critical density of the produced plasma. The ionization wave is understood as the wave expanding the boundary of the region of the medium where laser radiation absorption occurs.[18] Plasma heating behind the wave front is considered in the approximation of the absence of thermal energy conversion into hydrodynamic motion and intrinsic radiation energies. An approximate analytical solution for the velocity of such a wave can be constructed using two velocity scales. The first is the velocity D_h of the homogenization wave (H wave), behind the front of which a density-aligned plasma is formed. The duration of single-pore homogenization decreases with increasing temperature increase,[1,2] and therefore the H-wave velocity increases as the substance heats up. The second scale is the velocity D_c of the ionization wave in a continuous substance of subcritical density, which will henceforth be termed the ordinary ionization wave (OI wave). The OI-wave propagation is caused by an increase in the length of inverse bremsstrahlung absorption of laser radiation. The OI-wave velocity D_c at the time-constant laser intensity is given by a well-known self-similar solution,[18] according to which the OI-wave velocity decreases as the substance heats up.

Since the velocities D_h and D_c have opposite temperature dependences, there is an initial time interval $0 \le t \le t_d$ of low-temperature existence when the velocity D_c exceeds the velocity D_h. During this interval, the ionization wave velocity D is given by the H-wave velocity: $D = D_h$. At this stage, homogenization decelerates the ionization wave in a porous substance compared with its propagation in an equivalent continuous substance. As soon as the velocity D_c becomes less than the velocity D_h, ionization wave propagation is caused by the increasing depth of inverse bremsstrahlung absorption in the homogenized substance. The OI wave does not allow H-wave propagation ahead of itself, since all laser light is absorbed behind the OI-wave front and does not go beyond its boundary. Therefore, at $t \ge t_d$, the ionization wave velocity is given by the OI-wave velocity: $D = D_c$.

Let us determine the velocities D_c and D_h, as well as the time t_d, which constitute the essence of the above-described algorithm for constructing the solution for the ionization wave in a porous substance with subcritical density. The self-similar solution from Ref. 18 describes the propagation of a plane ionization wave under the action of a laser radiation flux with a constant intensity I on the surface of a half-space of motionless plasma in which the density ρ is less than the critical density and the electron temperature T is equal to the ion temperature. The solution was obtained using the inverse bremsstrahlung absorption coefficient of laser radiation in the form $\kappa = \kappa_0 \rho^2 / T^{3/2}$. The maintenance of the one-temperature plasma state and lack of movement during the entire period of wave propagation is supported. In Ref. 32, a simplified approach was used to describe the ionization wave velocity based on the self-similar solution from Ref. 18. The wave velocity was determined using the time scale of the self-similar solution for temperature, assuming that the temperature is uniformly distributed over the space behind the wave front. In the absence of material motion and any other losses

of plasma internal energy, the ionization wave velocity and plasma temperature are related by a simple balance equation $C_V D_c T\rho = I$ at a constant specific heat capacity C_V. In this paper, the approach from Ref. 32 described above is used to construct an analytical model. The expressions for wave velocities and temperatures differ from the corresponding expressions in Ref. 32 only by a constant coefficient, the introduction of which makes it possible to take into account the effect of the model approximations on the basis of experimental results. Then, the OI-wave velocity and the average temperature behind the OI-wave front are given by the following expressions:[18,32]

$$D_c[\,\mathrm{cm/s^{-1}}] \approx 9.5\times10^4\beta_c\frac{A^{7/5}}{Z^{6/5}}\left(\frac{\gamma-1}{Z+1}\right)^{3/5}\frac{I_{15}^{3/5}}{\rho^{7/5}\lambda_{\mu m}^{4/5}t_{ns}^{2/5}}, \quad (1)$$

$$T_c[\,\mathrm{keV}] \approx 63.1\left(\frac{\gamma-1}{Z+1}\right)^{2/5}\frac{I_{15}^{2/5}Z^{6/5}\rho^{2/5}\lambda_{\mu m}^{4/5}t_{ns}^{2/5}}{\beta_c A^{2/5}}, \quad (2)$$

where t_{ns} is the time measured in ns, $\lambda_{\mu m}$ is the laser radiation wavelength measured in μm, I_{15} is the laser intensity measured in 10^{15} W cm^{-2}, ρ is the plasma density measured in g cm^{-3}, Z and A are the charge and atomic number of plasma ions, γ is the adiabatic index, and β_c is the constant coefficient mentioned above. The OI-wave velocity increases when the laser wavelength and plasma density decrease. The OI-wave velocity and the temperature behind its front increase with laser intensity as $D_c \propto I^{3/5}$ and $T_c \propto I^{2/5}$. In contrast to the velocity, the temperature increases with increasing plasma density and laser wavelength. The velocity D_c decreases with time, according to the law $D_c \propto t^{-2/5}$. The temperature, by contrast, increases with time, according to the law $T_c \propto t^{2/5}$.

To find the H-wave velocity, the results of Refs. 1 and 2 related to the homogenization model of a low-density, high-porosity substance will be used. In Refs. 1 and 2, on the basis of a calculation of diffusion broadening of the homogenized plasma region as a result of ion–ion Coulomb scattering when the plasma flows from heated pore walls collide inside a pore, the following expression was obtained for the homogenization time of a single pore:

$$t_h(s) = \frac{\delta_0^2}{V_i^2\tau_{ii}} \approx 2.4\times10^{-11}\frac{Z^4\delta_0^2\rho}{A^{1/2}T^{5/2}}, \quad (3)$$

where V_i is the ion velocity of the colliding plasma flows, τ_{ii} is the time of ion–ion collisions, T is the temperature of the heated pore walls in keV, ρ is the average density of the porous substance in g cm^{-3}, and δ_0 is the average pore size in μm. The size δ_0 is related to the average thickness b_0 of the solid pore elements by the ratio[2]

$$\delta_0 = b_0\left(\frac{\rho_s}{\rho}\right)^{\alpha}, \quad (4)$$

in which ρ_s is the initial density of the pore wall material, and the fractal parameter α of the porous structure depends on the shape of solid elements and is equal to $(\nu+1)^{-1}$, where $\nu = 0$, 1, and 2 for flat (membranes), cylindrical (filaments), and spherical solid elements, respectively. For micro-sized porous substances having, as a rule, a mixed membrane–filament structure, $\alpha = 0.8$.

Homogenization in a substance with a structure of closed pores occurs sequentially as the density in a neighboring pore located closer to the laser-irradiated surface becomes less than the critical density. The H-wave velocity is defined as $D_h \approx \delta_0/t_h$. In the case of open pores, the initial homogenization occurs simultaneously in several pores located at a depth of geometric transparency from the irradiated surface, which, according to Ref. 2, is calculated as

$$L \approx 5\times10^{-4}\left(\frac{\rho_s}{\rho}\right)^{1-\alpha}\delta_0. \quad (5)$$

Further homogenization occurs sequentially from pore to pore, as in the case of a closed pore structure. Therefore, in a layer with open pore structure, the thickness of which significantly exceeds the length of geometric transparency, the H-wave velocity can be approximately determined in the same way as in a substance with closed pore structure. Then, using (3) and the energy balance equation

$$D_h C_V T_h \rho = I, \quad (6)$$

in which $C_V = (Z+1)k_B/(\gamma-1)Am_p$ is the specific heat capacity (k_B is the Boltzmann constant and m_p is the proton mass), we obtain the following expressions for the H-wave velocity and the average temperature behind its front:

$$D_h[\,\mathrm{cm/s^{-1}}] \approx 8.1\times10^6\beta_h\left(\frac{\gamma-1}{Z+1}\right)^{5/7}\frac{A^{6/7}I_{15}^{5/7}}{Z^{8/7}\delta_0^{2/7}\rho}, \quad (7)$$

$$T_h[\,\mathrm{keV}] \approx 1.3\times\beta_h^{-1}\left[\frac{Z^4A^{1/2}(\gamma-1)I_{15}\delta_0}{Z+1}\right]^{2/7}, \quad (8)$$

when

$$\delta_0 < L_0 \ll S. \quad (9)$$

Here, S is the thickness of the porous layer, and β_h is the constant coefficient that corrects for the use of a modeled description of the porous structure and takes into account the efficiency of laser energy absorption.

Let us consider the scope of applicability of the proposed H-wave model. The expression (3) for the homogenization time is derived in the approximation of collisions of plane flows of matter inside the pores. The use of this approximation is justified for substances with a large porosity exceeding values of the order of 0.95, at which a plasma flow will fly within a pore distances 5–10 times greater than the initial wall thickness. With a decrease in porosity, the result becomes sensitive to the geometry of the initial porous structure, which can apparently be correctly taken into account only through numerical calculation. To simplify the calculations, the expression (3) does not include an additional term associated with the primary expansion of the substance within a pore. This approximation is valid when the pore size significantly exceeds the ion mean free path. Both of the limitations noted here determine the range of applicability area of the H-wave model, as $\delta_0 \gg b_0$ and $\delta_0 \gg L_{ii}/3$. For the problem under consideration, both constraints are satisfied. First, the ratio of pore size to wall thickness for porous media used in modern experiments is several tens. Second, the ion mean free path for the density of the substances under consideration of several mg cm^{-3} and for the keV temperature of the produced plasma is about 0.1 μm. This is much smaller than the pore size of even

fine-pore media with a pore size of about 1 μm. Finally, the model can only be applied to sufficiently thick layers, the thickness of which significantly exceeds the geometric transparency length $S \gg L$. Using (5) with the value of fractal parameter $\alpha = 0.8$, it is found that this condition is satisfied for $S(\mu\text{m}) \gg 5(\rho_s/\rho)^{1/5}\delta_0$. At the ratio $\rho_s/\rho = 10^2$, the thicknesses of the layers of a fine-pore substance with a pore size $\delta_0 = 1$ μm and a large-pore substance with a pore size $\delta_0 = 10$ μm should significantly exceed 10 and 100 μm, respectively.

The homogenization model can be used outside the framework of the one-temperature approximation. In this case, the ion temperature should be used in (3). In Ref. 1, the effect of an excess of the ion temperature over the electron temperature was predicted as that due to the predominant transfer of internal energy into the thermal energy of ions in the process of homogenization. The effect was confirmed by experiments,[33] in which, for the considered highly porous media, the excess of the ion temperature was 30%–50%. However, in this paper, to simplify the calculations, the single-temperature plasma approximation is used. The influence of the ion temperature effect is implicitly taken into account through the coefficient β_h.

According to (7), the H-wave velocity increases with increasing laser intensity, as well as with decreasing density ρ and pore size δ_0. The temperature behind the H-wave front also increases with increasing laser intensity, but more weakly compared with the velocity D_h. It also increases with increasing pore size, but does not depend on density.

Equating the expressions (1) and (7), we obtain the following expression for the deceleration time t_d:

$$t_d[\text{ ns}] \approx 1.47 \times 10^{-5}\left(\frac{\beta_c}{\beta_h}\right)^{5/2}\left(\frac{Z+1}{\gamma-1}\right)^{2/7}\frac{A^{19/14}\delta_0^{5/7}}{Z^{1/7}\rho\lambda_{\mu\text{m}}^2 I_{15}^{2/7}}. \quad (10)$$

The deceleration time depends weakly on charge Z and laser intensity I. This time increases quite strongly with decreasing density ρ and laser wavelength λ, as well as with increasing pore size δ_0.

Thus, the solution for the ionization wave velocity in a porous substance of subcritical density is

$$D = D_h \times \begin{cases} 1, & \tau \le 1, \\ \tau^{-2/5}, & \tau \ge 1, \end{cases} \quad (11)$$

where $\tau = t/t_d$ is the current time normalized by the deceleration time t_d, which is given by the expression (10); the velocity D_h is given by the expression (7).

For practical applications, the duration of ionization wave propagation through a porous substance layer of given thickness is an important factor. Here, the degree of passage delay in the porous substance layer compared with an equivalent layer of continuous matter is a useful criterion. An elementary integration of the solution (11) makes it possible to find the analytical time dependence of the distance traveled by the ionization wave in a porous layer. As a result, the time t_p of wave passage through a layer of given thickness S as well as the time-depended temperature T behind the wave front are found:

$$T = T_h \times \begin{cases} 1, & \tau \le 1, \\ \frac{3}{5}\left(\frac{\tau}{\tau^{3/5}-\frac{2}{5}}\right), & \tau \ge 1, \end{cases} \quad (12)$$

$$t_p = t_c \times \begin{cases} \left(\frac{5}{3}\right)^{5/3}\tau_s^{-2/3}, & \tau_s \le 1, \\ \left(1+\frac{2}{3\tau_s}\right)^{5/3}, & \tau_s \ge 1. \end{cases} \quad (13)$$

Here, T_h is the temperature behind the H-wave front, which is given by the expression (8), and t_c and t_s are the durations of passage of the OI wave and H wave, respectively, through the layer of thickness S, respectively:

$$t_c = t_d\left(\frac{3}{5}\tau_s\right)^{5/3}, \quad (14)$$

$$t_s = \frac{S}{D_h}, \quad (15)$$

where $\tau_s = t_s/t_d$ [with td given by the expression (10)].

According to (13), the delay degree t_p/t_c increases with decreasing parameter $\tau_s = t_s/t_d \equiv S/(D_h t_d)$. If $\tau_s \le 1$, the ionization wave travels through the layer with the H-wave velocity. According to (7) and (10), this is the case for layers whose thicknesses are less than the limiting value

$$S_h[\mu\text{m}] \approx 1.2 \times 10^{-3}\frac{\beta_c^{5/2}}{\beta_h^{3/2}}\left(\frac{\gamma-1}{Z+1}\right)^{3/7}\frac{A^{31/14}\delta_0^{3/7}I_{15}^{3/7}}{Z^{9/7}\rho^2\lambda_{\mu\text{m}}^2}. \quad (16)$$

This value grows strongly (according to a quadratic law) with decreasing density and laser wavelength, and increases moderately with increasing pore size and laser intensity. The delay degree is greater the smaller the ratio of the layer thickness S to the distance that the H-wave travels during the deceleration time t_d. Therefore, *ceteris paribus*, the delay degree increases with decreasing layer thickness S and increasing deceleration time t_d. According to (13), the limiting case $\tau_s \to 0$ as $S \to 0$ corresponds to the ratio $t_p/t_c \to \infty$, i.e., the limiting case in which the OI wave does not have the ability to propagate in the layer of porous matter. With increasing layer thickness, the delay degree decreases in the boundless layer $S \to \infty$, which means $\tau_s \to \infty$, $t_p/t_c \to 1$, which, in fact, means OI-wave propagation.

III. COMPARISON WITH EXPERIMENT

The goal of this section is to establish the values of the coefficients β_h and β_c in the expressions (1) and (7) on the basis of data on laser-driven ionization wave velocity in a subcritical porous substance measured in experiments that we were able to find in the literature. Table I shows the data on these experimental conditions and the wave velocity determined as the ratio of the porous layer thickness S to the time $t$ex of wave arrival at the rear side of the layer. The experiments were performed with nanosecond laser beams that provides intensities in the range of $(3–8) \times 10^{14}$ W cm^{-2} at radiation wavelengths in the range of 0.35–0.53 μm. The pulses with simple temporal profiles such as square- or trapeze-like were used. In all the experiments, porous substances based on light chemical elements with average values of charge and atomic number of about $Z = 4$ and $A = 8$, respectively, were used. The average substance density in all experiments ranged from 4.5 to 12 mg cm^{-3}.

With the exception of the JLF experiment, a fine-pore substance with an average pore size of about 1 μm was studied in all experiments. In the JLF experiment, a large-pore substance with a pore size of 25 μm was used. The Shenguang III experiment differed from the others in the scheme of target irradiation, where each of the layer surfaces was irradiated by a pair of obliquely incident laser beams. All other experiments were performed with one-side irradiation by a single normally incident beam.

In all experiments, with the exception of the LIL experiment, the laser beam radius was significantly smaller than the layer thickness. Therefore, comparison of the 1D solution (11) with the experimental data under consideration is possible only when account is taken of corrections describing the 2D effects of laser beam interaction with target. These corrections, first of all, should describe energy losses caused by substance motion in the transverse direction with respect to the H-wave and OI-wave direction, which still coincides with the direction of laser beam incidence. An approximate way to introduce such corrections is to consider a 2D ionization wave in the form of a hybrid wave with different front propagation velocities in the longitudinal and transverse directions. In the longitudinal direction, a wave front with cross section equal to that of the laser beam propagates with the velocity of a plane ionization wave. In the transverse direction, the wave front is formed as a result of transverse shock wave propagation. Its surface is the lateral surface of a truncated cone of height equal to the distance travelled by the plane ionization wave. The small base of the cone represents the forward wave's front and has a radius equal to the laser beam radius. The large base of the cone is located on the irradiated surface. Its radius is equal to the sum of the laser beam radius and the distance that the transverse shock wave supported by the H wave or OI wave travels to a given moment. A description of such a hybrid wave can be approximately constructed by distributing the flow of input laser energy over the entire surface of the wave front. This means replacing the laser pulse intensity I by an effective value I^*, reduced in comparison with I by the ratio of the cross-sectional area of the laser beam to the surface area of the hybrid wave front. Using this approach, for the velocity of the longitudinal OI wave or H wave as part of a hybrid wave, one can use the expressions (1) and (7), respectively, for the 1D OI wave or 1D H wave, but with the laser intensity of the incident laser beam I replaced by the effective intensity I^*:

$$D_{h*} = D_h\left(\frac{I_{h*}}{I}\right)^{5/7}, \quad D_{c*} = D_c\left(\frac{I_{c*}}{I}\right)^{3/5}. \tag{17}$$

We can then apply the algorithm used in Sec. II to construct a solution based on OI-wave and H-wave competition by means of the deceleration time t_{d*} determined from the equality of the velocities of these waves. The hybrid wave front area can be determined using the method of successive approximations when the velocities of the longitudinal OI and H waves are calculated using the expressions (1) and (7) for the 1D OI and 1D H waves, respectively, and the velocities of the corresponding transverse shock waves are calculated from the temperatures behind the fronts of the 1D OI and 1D H waves. Then, at $S > R$, the effective intensity I^* for the H wave or OI wave during the period of its propagation through a layer of thickness S is given by

$$I_{(h,c)*} = I\left(1 + \frac{1}{6}\frac{S}{R}\frac{D_{s(h,c)}}{D_{h,c}}\right)^{-2}, \tag{18}$$

where $D_{s(h,c)}$ is the velocity of the transverse shock wave initiated by the H wave or OI wave.

The velocities of the transverse shock waves are calculated according to the formula $D_{s(h,c)} = [2(\gamma-1)C_V T_{h(c)}/(\gamma+1)]^{1/2}$, where the temperatures behind the fronts of the 1D OI and 1D H waves, T_c and T_h, are determined by the formulas (2) and (8). This procedure gives the following expressions for the velocities:

$$D_{s(c)} = 2.3\times10^8\frac{Z^{3/5}(Z+1)^{3/10}(\gamma+1)^{1/2}(\gamma-1)^{1/5}}{A^{7/10}\beta_c^{1/2}}(\rho I_{15}\lambda_{\mu m}^2 t_{ns})^{1/5}, \tag{19}$$

$$D_{s(h)} = 2.55\times10^7\frac{(\gamma+1)^{1/2}(\gamma-1)^{1/7}(Z+1)^{5/14}Z^{4/7}\delta_0^{1/7}I_{15}^{1/7}}{A^{3/7}\beta_h^{1/2}}. \tag{20}$$

In further calculations, the following expressions derived from (1) and (7) and from (19) and (20) at $\gamma = 5/3$ are used, with the values $Z = 4$ and $A = 8$ corresponding to the porous substances studied in experiments:

$$D_c[\mathrm{cm/s^{-1}}] \approx 9.9\times10^4\frac{\beta_c I_{15}^{3/5}}{\rho^{7/5}\lambda_{\mu m}^{4/5}t_{ns}^{2/5}}, \tag{21}$$

$$D_{s(c)}[\mathrm{\ cm/\ s}] \approx 3\times10^8\frac{(\rho I_{15}\lambda_{\mu m}^2 t_{ns})^{1/5}}{\beta_c^{1/2}}, \tag{22}$$

$$D_h[\mathrm{cm/s^{-1}}] \approx 2.35\times10^6\frac{\beta_h I_{15}^{5/7}}{\delta_0^{2/7}\rho}, \tag{23}$$

$$D_{s(h)}[\mathrm{cm/s^{-1}}] \approx 6.3\times10^7\frac{\delta_0^{1/7}K_p^{1/7}I_{15}^{1/7}}{\beta_h^{1/2}}. \tag{24}$$

Using (21)–(24), we then obtain the following expressions for the effective intensity in the cases of an OI wave and an H-wave, respectively:

$$I_{c*} = I\left(1 + 2.5\times10^2\frac{S}{R}\frac{\rho^{8/5}\lambda_{\mu m}^{6/5}t_{ns}^{3/5}}{I_{15}^{2/5}\beta_c^{3/2}}\right)^{-2}, \tag{25}$$

$$I_{h*} = I\left(1 + 4.4\frac{S}{R}\frac{\delta_0^{3/7}\rho}{\beta_h^{3/2}I_{15}^{4/7}}\right)^{-2}. \tag{26}$$

The greater the 2D effect, the smaller is the ratio I^*/I. According to (25) and (26), in both cases, this effect becomes greater with increasing density ρ and with decreasing nominal laser intensity I and decreasing ratio R/S. In addition, in the case of an OI wave, the 2D effect increases with increasing laser wavelength and wave passage time. In the case of an H wave, the 2D effect increases with increasing pore size.

Taking into account the relationship between the statement of the theoretical model and the experimental conditions, a direct comparison of theoretical and experimental results will be carried out for

TABLE I. Experimental conditions.[a]

Experiment	I (10^{14} W cm^{-2})	τ_L (ns)	λ (μm)	R (μm)	S (μm)	ρ (mg cm^{-3})	δ_0 (μm)	t_{ex} (ns)	D_{ex} (10^7 cm s^{-1})	Notes
Gekko-12[21]	3	3	0.35	100	500	10	~1	1.7	2.9	Normal incidence of third-harmonic Nd-laser beam
LIL[6]	4	2.7	0.35	1000	950	10	~1	1.6	6	
PALS[22,23]	4	0.32	0.44	150	380	4.5	~2	0.5	7.6	Normal incidence of third-harmonic I-laser beam
PALS[22,23]	4	0.32	0.44	150	400	9	~2	1.3	3.1	
JLF[24]	3	2	0.53	100	442	12	25	1.4	3.16	Normal incidence of second-harmonic Nd-laser beam
Shenguang III prototype[25]	4–8	1	0.35	250	800/2	10–12	~1	···	3–3.5	Oblique incidence of two beams of third-harmonic Nd-laser radiation

[a] I is the laser intensity (at half-maximum), τ_L is the pulse duration, λ is the laser wavelength, S is the layer thickness, ρ is the average substance density, δ_0 is the average pore size, t_{ex} is the time of wave arrival at the rear side of the layer, and $D_{ex} = S/t_{ex}$ is the average ionization wave velocity.

the Gekko-12 and LIL experiments, as well as for the PALS experiment with a layer of substance density 4.5 mg cm^{-3}. In all these experiments, the layers have a thickness significantly larger than the geometric transparency length, which is a necessary condition for the existence of an H wave. In addition, the layer thicknesses and pulse durations in these experiments corresponded to a wave passage time through the layer that was less than (or close to) the laser pulse duration. The data related to these experiments, which will be referred to as the basic ones, are presented in the first three rows of Table I. For the remaining experiments in Table I, a partial comparison will be carried out, together with discussion of several results of these experiments that are due to their specific conditions.

First of all, we note that the ionization wave velocities in the basic experiments differed significantly, which was due to the differences in experimental conditions. Thus, in the LIL experiment, the wave velocity was more than twice that in the Gekko-12 experiment. These experiments differed in their ratio of layer thickness to beam radius. This parameter in the LIL experiment ($S/R = 1$) was one-fifth of that in the Gekko-12 experiment ($S/R = 5$). In the PALS (4.5 mg cm^{-3}) experiment, the ionization wave velocity significantly exceeded not only the Gekko-12 result, but also the LIL result. The PALS (4.5 mg cm^{-3}) experiment was distinguished by the fact that the density of the porous substance was 2.2 times smaller than that in the Gekko-12 and LIL experiments.

The comparison with the results of the basic experiments presented below demonstrates that the model not only qualitatively but also quantitatively describes the experimental results with the same pair of coefficients β_c and β_h, whose values are close to 1: $\beta_c = 3/4$ and $\beta_h = 2/3$. It is important to note that the model describes significant differences in the ionization wave velocity caused by various physical effects. As already noted, the coefficient β_h corrects for, among other things, the uncertainty related to absorbed laser energy fraction. Among the results of the experiments under consideration, the absorption efficiency was not discussed. However, with the help of several other papers mentioned in Sec. I, it is possible to conclude that about 15% of laser energy is lost due to linear reflection from the solid elements of the pores and about 10% lost is due to nonlinear stimulated Brillouin scattering in the produced plasma. Therefore, the absorbed energy fraction in a porous substance can be considered to lie in the range 0.7–0.75. Bearing in mind the dependence of the H-wave velocity on the intensity as $D_h \propto I^{5/7}$, this range of values of the absorbed energy fraction leads to a decrease in the velocity by a factor of 0.8–0.85.

It should be noted that the constancy of the coefficients β_c and β_h is substantiated below by comparing the model with experiments in which laser pulses of simple temporal shapes such as square- or trapeze-like were used. In the case of pulses with a complex temporal shape, this "universality" of β_c and β_h will be violated, because the dependence of laser pulse intensity on time will make its own contribution to the nonstationarity of the solution. In this case, a simple model similar to that developed in this paper can be useful for understanding the scaling relationships of ionization wave dynamics in individual intervals of the laser pulse with characteristic intensity values.

The ionization wave characteristics calculated according to the 1D solution and 2D corrections with the above-mentioned values of β_c and β_h for the basic experiments are shown in Table II. In the Gekko-12 experiment, the measured time for passage of the ionization wave through a layer of fine-porous substance with a thickness of 500 μm was 1.7 ns.[21] This time corresponds to an average wave velocity $D_{ex} \approx 2.9 \times 10^7$ cm s^{-1} (290 μm ns^{-1}), as shown in Table I. In the accompanying 2D numerical calculations of Ref. 21, the wave passage time through an equivalent layer of continuous matter was about 0.7 ns, which corresponds to an average OI-wave velocity of 7.1×10^7 cm s^{-1} (710 μm ns^{-1}). On the basis of these data, a combined (experimental–calculated) value of the delay degree of 2.5 was established in Ref. 21. The 1D solution for the Gekko-12 experiment gives values of the 1D H-wave velocity and 1D OI-wave average velocity of $D_h \approx 6.6 \times 10^7$ cm s^{-1} and $D_{ca} \approx 1.25 \times 10^8$ cm s^{-1}, respectively (Table II). The 1D H-wave inhibits the ionization wave for a time $t_d \approx 0.55$ ns. The calculated time of ionization wave passage was $t_p \approx 0.76$ ns, which is close to the deceleration time t_d. Thus, the average ionization wave velocity $D_a \approx 6.4 \times 10^7$ cm s^{-1} is slightly less than the H-wave velocity ($D_h \approx 6.6 \times 10^7$ cm s^{-1}). The delay degree D_{ca}/D_h for the 1D ionization wave is 1.93.

TABLE II. Model results.[a]

Experiment	1D solution					2D model					
	D_h (10^7 cm s^{-1})	D_{ca} (10^7 cm s^{-1})	t_d (ns)	t_p (ns)	D_a (10^7 cm s^{-1})	D_{h*} (10^7 cm s^{-1})	D_{ca*} (10^7 cm s^{-1})	t_{d*} (ns)	t_{p*} (ns)	D_{ca*}/D_{h*}	D_{a*} (10^7 cm s^{-1})
Gekko-12	6.6	12.5	0.55	0.76	6.4	3	6.8	1.57	1.67	2.3	3
LIL	8.1	11.2	0.62	1.53	6.2	6.8	9.7	0.67	1.9	1.6	5.1
PALS (4.5 mg cm^{-3})	15	95	1.17	0.25	15	9.8	76	2.4	0.39	7.8	9.8

[a] D_h is the 1D H-wave velocity, D_{ca} is the 1D OI-wave average velocity, t_d is the deceleration time for the 1D ionization wave, t_p is the passage time of tjhe 1D ionization wave, t_p/t_c is the delay degree for the 1D ionization wave, D_a is the average velocity of the 1D ionization wave, D_{h*} is the 2D H-wave velocity, D_{ca*} is the 2D OI-wave average velocity, t_{d*} is the deceleration time for the 2D ionization wave, t_{p*} is the passage time of the 2D ionization wave, D_{ca*}/D_{h*} is the delay degree for the 2D ionization wave, and D_{a*} is the average velocity of the 2D ionization wave.

Under the conditions of the Gekko-12 experiment[21] with the ratio $S/L = 5$, the 2D corrections leads to a significant decrease in the effective laser intensity I^* compared with the nominal one, especially for the H wave: $I_{c*} = 0.57I$ and $I_{h*} = 0.32I$. As a consequence, the velocity of the 2D H-wave decreases by a factor of 2.2 to the value $D_{h*} \approx 3 \times 10^7$ cm s^{-1}, which practically coincides with that measured in the experiment (2.9×10^7 cm s^{-1}). The velocity of the 2D OI wave decreases to a value of $D_{ca*} \approx 6.8 \times 10^7$ cm s^{-1}. Thus, the ionization wave in the Gekko-12 experiment has a pronounced 2D character. The 2D H wave decelerates the ionization wave during practically the entire passage time: the deceleration time is $t_d \approx 1.57$ ns and the passage time is $t_p \approx 1.67$ ns. The calculated delay degree is 2.3, which is very close to the value of 2.5 presented in Ref. 21.

The calculated 1D velocities for the LIL experiment do not significantly change compared with those calculated for the Gekko-12 experiment. The 1D H-wave velocity increases in comparison with the Gekko-12 case owing to an increase in laser intensity by 4/3 times (from 3×10^{14} to 4×10^{14} W cm^{-2}) to a value of $D_h = 8.1 \times 10^7$ cm s^{-1} in accordance with the dependence $D_h \propto I^{5/7}$ [see (7)]. Despite the increase in laser intensity, the 1D OI-wave average velocity $D_{ca} = 1.1 \times 10^8$ cm s^{-1} decreases slightly compared with the Gekko-12 case. This is explained by the fact that the OI wave with decreasing velocity contributes more significantly to the ionization wave velocity than in the Gekko-12 experiment, in which the layer thickness of 500 μm is half that in the LIL experiment. The 1D H wave inhibits the ionization wave for a time $t_d \approx 0.62$ ns. The 1D ionization wave passage time through the layer of thickness 1000 μm is $t_p \approx 1.53$ ns. This time, unlike that in the Gekko-12 experiment, significantly exceeds the deceleration time t_d, and so the deceleration effect in the LIL experiment is less pronounced. The delay degree for the 1D ionization wave is 1.65 (1.93 for the Gekko-12 experiment), and the ionization wave velocity $D_h = 6.2 \times 10^7$ cm s^{-1} is less than the H-wave velocity (8.1×10^7 cm s^{-1}).

In the LIL experiment with a focal spot radius of 1000 μm, i.e., ten times larger than that in the Gekko-12 experiment, the role of the 2D effect is much less pronounced than in the Gekko-12 experiment. At the ratio $S/L = 1$, the decrease in the effective laser intensity I^* compared with the nominal one is only about 1.3 times, for both the H wave and the OI wave. As a result, the velocities of the 2D waves decrease by only about 1.17 times to values of $D_{h*} = 6.8 \times 10^7$ cm s^{-1} and $D_{ca*} \approx 9.7 \times 10^7$ cm s^{-1}. The ionization wave in the LIL experiment is close to being 1D. The deceleration time for the 2D ionization wave is $t_{d*} \approx 0.67$ ns and the passage time through a 1000 μm layer is $t_{p*} \approx 1.9$ ns. The delay degree for the 2D wave is 1.6, i.e., practically the same value as in the case of the 1D approximation. The calculated 2D ionization wave average velocity, $D_{a*} = 5.1 \times 10^7$ cm s^{-1}, differs slightly from the measured value (6×10^7 cm s^{-1}).[6]

The velocities of the 1D OI wave and 1D H wave increase with decreasing density ρ as $D_h \propto \rho^{-1}$ and $D_c \propto \rho^{-7/5}$ [see (1) and (7)]. Therefore, in the PALS (4.5 mg cm^{-3}) experiment, the calculated 1D-wave velocities significantly exceed the values for the Gekko-12 and LIL experiments, in which the porous substance density is 10 mg cm^{-3}. The 1D H-wave velocity is $D_h = 1.5 \times 10^8$ cm s^{-1}, and the 1D OI-wave average velocity is $D_c = 9.5 \times 10^8$ cm s^{-1}. In the layer of thickness 380 μm, the 1D H wave inhibits the ionization wave during the entire passage time of $t_p \approx 0.25$ ns (the deceleration time t_d in the boundless layer is 1.17 ns). Therefore, the 1D ionization wave velocity is equal to the H-wave velocity. The delay degree is 6.3, which is significantly greater than in the Gekko-12 and LIL experiments. In the PALS (4.5 mg cm^{-3}) experiment with a focal spot radius of 150 μm and a layer thickness of 380 μm, the ratio $S/R = 2.5$ is an intermediate value between those of the LIL and Gekko-12 experiments. Under such conditions, taking into account the significantly larger velocities of 1D waves, the role of the 2D effect is small. It is only slightly greater than in the LIL experiment. The effective laser intensities are $I_{c*} = 0.86I$ for the OI wave and $I_{h*} = 0.71I$ for the H wave. As a result, the velocities of 2D waves decrease to values $D_{h*} = 9.8 \times 10^7$ cm s^{-1} and $D_{ca*} \approx 7.6 \times 10^8$ cm s^{-1}. The 2D H wave slows down the ionization wave during the entire passage time $t_{p*} \approx 0.39$ ns (the deceleration time t_{d*} in a boundless layer is 2.4 ns). Therefore, the 2D ionization wave velocity is equal to the 2D H-wave velocity. The delay degree is 7.8, which is significantly larger than in the Gekko-12 and LIL experiments. The calculated ionization wave velocity of 9.8×10^7 cm s^{-1} exceeds the measured value of 7.6×10^7 cm s^{-1}.[22,23] This difference is apparently due to the fact that in the PALS (4.5 mg cm^{-3}) experiment, the pulse duration is less than the wave passage time (0.5 ns), and hence the wave path in a small part of the layer is a damping one.

Thus, under the conditions of the Gekko-12 and PALS experiments with relatively thin porous layers, the propagation times of the ionization wave are shorter than the deceleration times t_d.

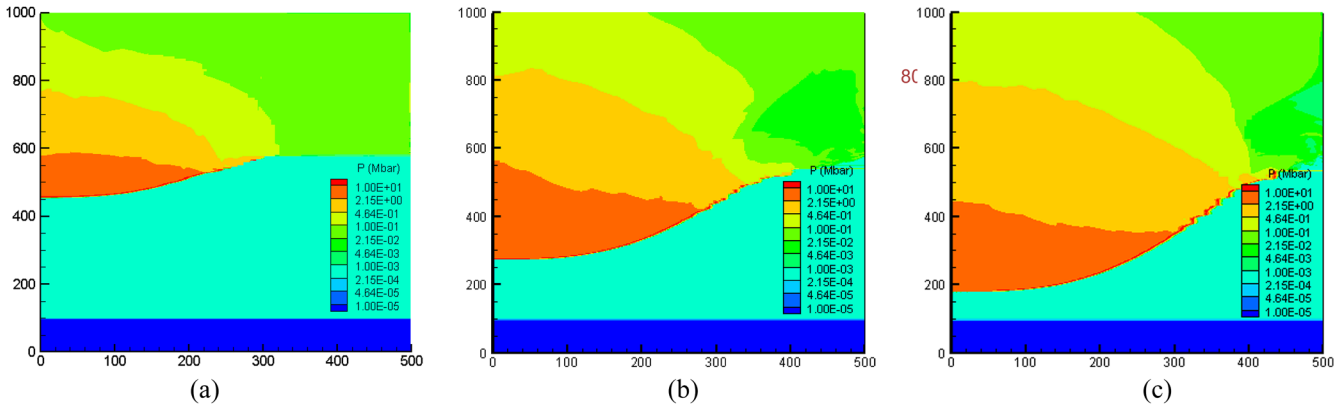

FIG. 1. Pressure isoline distributions at moments of time 0.5, 1, and 1.3 ns (from left to right) after the beginning of the laser pulse. The porous layer initially occupies the area from 100 to 600 μm.

Ionization waves propagate in a stationary mode with constant H-wave velocities. Under the conditions of the LIL experiment with an extended porous layer, the ionization wave propagates for a sufficiently long time, exceeding the deceleration time. That is to say, in this experiment, the nonstationarity of the solution associated with the contribution of the OI wave is manifested. The result of such a contribution of non-stationarity is that the wave propagation velocity turns out to be less than the H-wave velocity.

In Figs. 1 and 2 as an illustration, the results are shown of numerical simulations of 2D ionization waves under the conditions of the Gekko-12 experiment. The calculations were performed using the NUTCY-F code, which is one of the versions of the NUTCY Eulerian code[34,35] for the modelling of laser–plasma hydrodynamics in an axisymmetric geometry. The NUTCY-F code uses the equation of state of partially homogenized plasma. Such an equation of state takes into account the contributions to pressure from only the homogenized part of matter. The nonhomogenized plasma, which participates in the turbulent motion inside the pores, does not contribute to the pressure. The partial density of a homogenized plasma at a given moment of time at a given point in space is calculated using the homogenization model,[36] with the homogenization time of an individual pore given by the expression (3). Figure 1 shows the pressure isoline distributions at three moments of time 0.5, 1, and 1.3 ns after the beginning of the laser pulse. A layer of fine-pore substance ($\delta_0 = 1$ μm) with a density of 10 mg cm^{-3} initially occupies the area from 100 to 600 μm. Figure 2 shows the pressure (black line) and temperature (red line) distributions along the optical axis of the laser beam at the moment of time 1.3 ns. The average velocity of the ionization wave along the optical axis is about $D_h = 3.2 \times 10^7$ cm s^{-1}, which practically coincides with the experimental result. The velocity of the transverse shock wave is about (2.3–2.5) $\times 10^7$ cm s^{-1}.

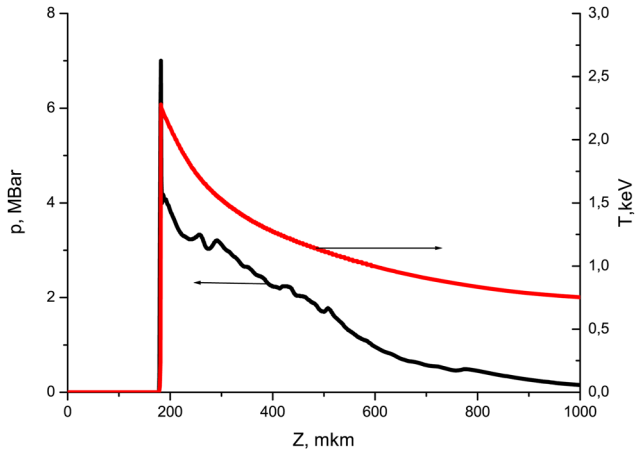

FIG. 2. Pressure (black line) and temperature (red line) distributions along the optical axis of the laser beam at the moment of time 1.3 ns. The porous layer initially occupies the area from 100 to 600 μm.

Now, with using the theoretical model, let us discuss the results of the JLF and Shenguang III experiments, as well as the PALS (9 mg cm^{-3}) experiment with a layer of porous substance of density 9 mg cm^{-3}. In the JLF experiments, the measured wave passage time through a 442 μm thickness layer of large-pore substance with a pore size of 25 μm is 1.4 ns. This time corresponds to the ionization wave average velocity $D_{ex} \approx 3.16 \times 10^7$ cm s^{-1} (316 μm ns^{-1}) shown in Table I. The length of geometric transparency of such a substance, according to the expression (5), can be estimated as $L \approx 300$ μm. The remaining thickness $S - L = 140$ μm exceeds the average pore size by 5.6 times, which makes it possible to apply the developed model to describe ionization wave propagation in this part of the layer. Compared with the Gekko-12 experiment, the 1D OI-wave velocity decreases owing to an increase in laser wavelength and an increase in density ρ, and the H-wave velocity decreases owing to an increase in pore size and also an increase in density. The 1D OI-wave and 1D H-wave velocities are $D_{ca} \approx 1.1 \times 10^8$ cm s^{-1} and $D_h \approx 2.2 \times 10^7$ cm s^{-1}, respectively, The significant delay degree of about 5 is the reason why the velocity of the 1D ionization wave is equal to the 1D H-wave velocity. The 1D ionization wave travels through a part of the layer with a thickness of $S - L \approx 140$ μm during the time of 0.64 ns.

The 2D corrections give values of the effective laser intensity $I_{c*} = 0.77I$ for the OI wave and $I_{h*} = 0.25I$ for the H wave. The 2D effect is very significant for the H wave. The 2D OI-wave and 2D H-wave velocities decrease (the latter especially strongly) to values of $D_{c*} \approx 8.8 \times 10^7$ cm s^{-1} and $D_{h*} \approx 0.85 \times 10^7$ cm s^{-1}. The delay degree of 2D ionization wave increases to 10.3. The ionization wave velocity is equal to the 2D H-wave velocity. Hence, the wave passage time of a layer with a thickness of 140 μm is 1.6 ns. This time is close to the experimental value (1.4 ns), and in terms of the layer thickness of 440 μm it gives a wave velocity of about 2.75×10^7 cm s^{-1} (3.16×10^7 cm s^{-1} in the experiment[24]).

In the PALS (9 mg cm^{-3}) experiment, the measured ionization wave passage time through a layer of thickness 400 μm is 1.4 ns, which significantly exceeds the duration of the laser pulse (320 ps).[22,23] This means that the wave propagates over most of the layer as a damped one. In fact, the conditions of the PALS (9 mg cm^{-3}) experiment differ from those of the PALS (4.5 mg cm^{-3}) experiment, only by the twofold-increased density ρ. The laser beam is the same. The layer thickness of 400 μm is only 20 μm greater than that in the PALS (4.5 mg cm^{-3}) experiment. A twofold increase in density leads to the same decrease in the 1D H-wave velocity, and a 2.64-fold decrease in the 1D OI-wave velocity compared with the PALS (4.5 mg cm^{-3}) experiment. These velocities during the pulse action are $D_h \approx 7.5 \times 10^7$ cm s^{-1} and $D_c \approx 2.6 \times 10^8$ cm s^{-1}. The delay degree is 3.55. The velocities of 2D waves decrease to values of $D_{h*} \approx 5.8 \times 10^7$ cm s^{-1} and $D_{c*} \approx 2.3 \times 10^8$ cm s^{-1}. The delay degree for the 2D ionization wave increases to 3.9. The 2D ionization wave propagates with the H-wave velocity, and during the laser pulse action it travels through part of the layer with a thickness of 185 μm. In the experiment, the ionization wave travels through a layer of thickness 400 μm with a velocity of 2.85×10^7 cm s^{-1}. Thus, it can be concluded that the damped ionization wave after laser pulse termination traverses a distance of 225 μm in the PALS (9 mg cm^{-3}) experiment with an average velocity of 2.05×10^7 cm s^{-1}.

In the Shenguang III experiments, each surface of a layer of fine-pore substance is irradiated by a pair of laser beams. The layer thickness is 800 μm. The density of the substance is 10 or 12 mg cm^{-3}. Each beam has an elliptical cross section and hits the layer surface at an angle of 45°. On the surface, each beam has a circular cross section of radius 250 μm. The area of overlap of the beams on the layer surface is relatively small and its square is about one-sixth of a single beam square. The intensity of each beam on the layer surface is about 4×10^{14} W cm^{-2}. The pulse duration is about 1 ns. In the experiment with a substance density of 10 mg cm^{-3}, the ionization wave propagates to a depth of 300–350 μm during the action of the laser pulse (1 ns).[25] This distance is less than half the thickness of the layer. Both the OI wave and the H wave propagate in the direction of laser beam incidence. Hence, the ionization wave passage time through a layer is determined by the wave velocity component directed normally to the layer surface, which is related to the total wave velocity through the cosine of the angle of 45°.

To analyze the results of the experiments with the radiation scheme described above, calculations using the 2D ionization wave model are carried out for two cases with intensities of 4×10^{14} and 8×10^{14} W cm^{-2}, respectively. In the first case, the ionization wave velocity corresponding to the distance of 350 μm is about 4×10^7 cm s^{-1}, which is in satisfactory agreement with the experimental result. In the second case, the velocity is 7.6×10^7 cm s^{-1}, which is twice the experimental result. Hence, it can be concluded that the two-beam scheme of irradiation of the layer surface used in the Shenguang III experiment, at least from the point of view of ionization wave initiation, is equivalent to irradiation with one beam.

IV. LASER-DRIVEN GENERATION OF A PLANE IONIZATION WAVE WITH PREDICTED VELOCITY IN A LAYER OF SUBCRITICAL POROUS SUBSTANCE OF GIVEN THICKNESS

The good agreement of the theoretical model with experimental results is an argument to apply the analytical solution (1)–(7) to establish conditions for generating a flat laser-supported ionization wave in a layer of porous substance of finite thickness. That is to say, the plane ionization wave is, first of all, of interest for investigations related to ICF and EOS determination, where it is necessary to know the parameters of the laser beam (pulse energy, pulse duration, radiation wavelength, and focal spot radius) that initiates the propagation of a plane ionization wave in a layer of porous material with specified values of layer thickness, average substance density, and structural parameters during the entire duration of the laser pulse. Obviously, a laser pulse with minimal energy (optimal pulse) should have duration equal to the time of wave passage through the layer. As a criterion for generating such a plane wave, a beam diameter equal to the layer thickness will be considered for the optimal pulse. Further analysis will be carried out using the solutions (11) and (13), taking into account (1), (7), and (10) for a fine-pore substance with a pore size of 1 μm at atomic number $A = 8$ and charge $Z = 4$, which corresponds to most of the experiments in Table I.

Figures 3 and 4 show the dependences of the delay degree t_p/t_c (a) and wave passage time t_p (b) on layer thickness S for two wavelengths (0.53 and 0.35 μm) and three densities ρ (10, 5, and 2 mg cm^{-3}) at laser intensities of 10^{14} W cm^{-2} (Fig. 3) and 10^{15} W cm^{-2} (Fig. 4). The passage time t_p, equal to the optimal pulse duration, increases with decreasing laser intensity and wavelength, and increases with increasing density ρ. For example, at a laser intensity of 10^{14} W cm^{-2} and wavelength 0.35 μm for a layer of thickness 1000 μm, the pulse durations are 4.75 and 1.65 ns at the densities of 10 and 5 mg cm^{-3}, respectively. At a wavelength of 0.53 μm, these values increase to 7.4 and 1.91 ns, respectively. At a laser intensity of 10^{15} W cm^{-2} and wavelength of 0.35 μm for a layer with the same thickness of 1000 μm, the pulse durations are 0.67 and 0.32 ns at densities of 10 and 5 mg cm^{-3}, respectively. The delay degree t_p/t_c, as already discussed in Sec. II, all other things being equal, decreases with increasing layer thickness. At a layer thickness of 1000 μm, the ratio t_p/t_c is close to 1 over the entire wide range of changes in the parameters of the problem. Note that the dependences of the passage time t_p at the lowest density of 2 mg cm^{-3} are not distinguished in the layers of thickness less than 1000 μm for both wavelengths in both cases of laser intensity. At such a low density, the layer thickness S_h for which the H wave decelerates the OI wave during the entire passage time [see (16)] is greater than 1000 μm. The ionization wave propagates with the H-wave velocity, which does not depend on thje laser wavelength.

For the same values of substance density, laser intensity, and wavelength as in Figs. 3–6 show the dependences of the optimal pulse energy (the duration of the pulse is given by the data in Figs. 3

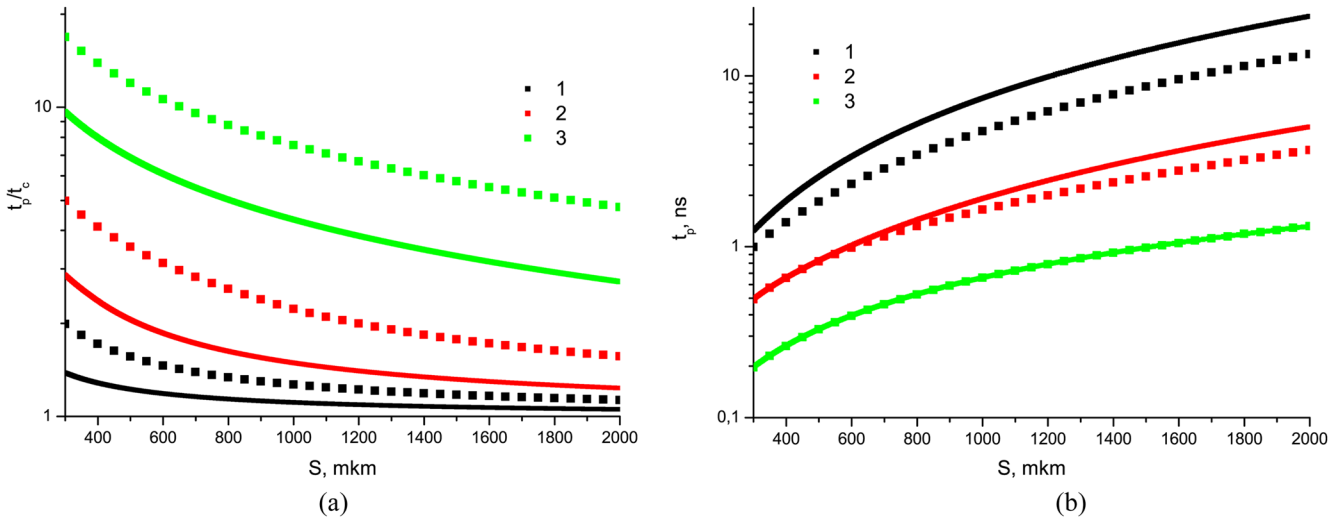

FIG. 3. Dependences of delay degree t_p/t_c (a) and ionization wave passage time t_p (b) on layer thickness S at a laser intensity of 10^{14} W cm^{-2} for two wavelengths 0.53 μm (solid lines) and 0.35 μm (dotted lines) and for three densities 10 mg cm^{-3} (black lines), 5 mg cm^{-3} (red lines), and 2 mg cm^{-3} (green lines).

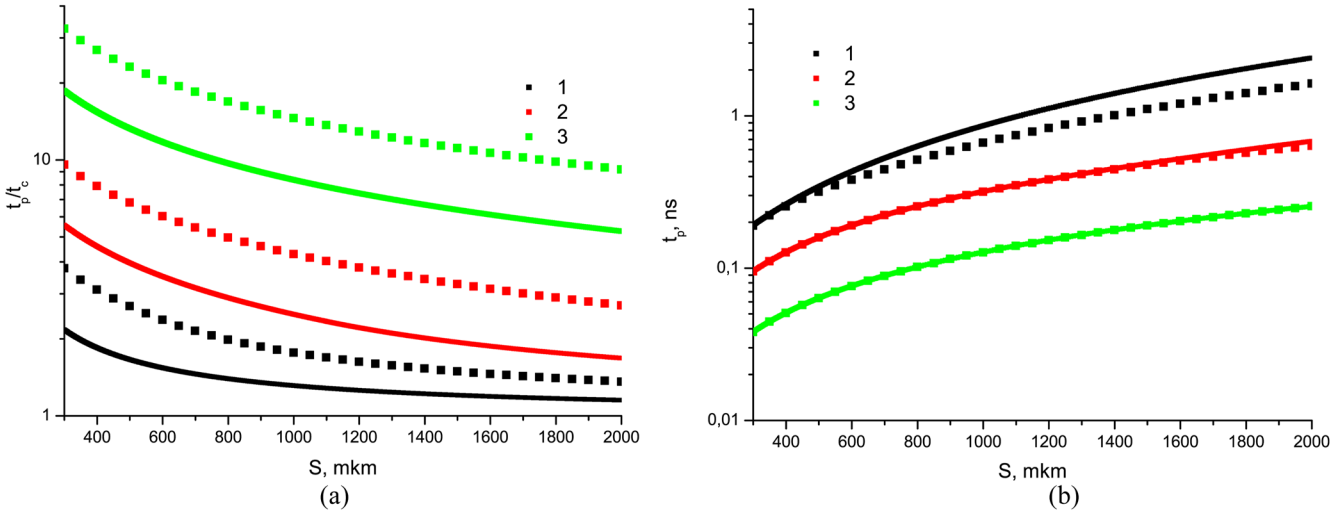

FIG. 4. Dependences of delay degree t_p/t_c (a) and ionization wave passage time t_p (b) on layer thickness S at a laser intensity of 10^{15} W cm^{-2} for two wavelengths 0.53 μm (solid lines) and 0.35 μm (dotted lines) and for three densities 10 mg cm^{-3} (black lines), 5 mg cm^{-3} (red lines), and 2 mg cm^{-3} (green lines).

and 4, and the beam diameter is equal to the layer thickness) and average ionization wave velocity on the layer thickness S.

The optimal pulse energy, naturally, increases with layer thickness. At a given layer thickness, the energy increases with increasing density, laser intensity, and wavelength. For a layer of thickness 1000 μm, the optimal pulse with intensity 10^{14} W cm^{-2} and wavelength 0.35 μm has an energy of 500 J at a density ρ = 2 mg cm^{-3} (Fig. 5), whereas the optimal pulse with intensity 10^{15} W cm^{-2} and wavelength 0.53 μm has an energy of 6 kJ at a density ρ = 10 mg cm^{-3} (Fig. 6). The dependences of the average wave velocity for the lowest density of 2 mg cm^{-3} are not distinguished in layers of thickness less than 1000 μm for both wavelengths in both cases of laser intensity. Accordingly, the dependences of the optimal pulse energy are also not distinguished for the lowest density of 2 mg cm^{-3}. As mentioned above, this is because the ionization wave propagates with the velocity of the H-wave, which decelerates the ionization wave at such a small substance density during the entire passage time. At the higher densities of 5 mg cm^{-3} and, especially, 10 mg cm^{-3}, the effect of a decreasing wave velocity with increasing layer thickness is manifested. This decrease is stronger, the longer is the laser wavelength. This happens because at such large densities, the ionization wave deceleration by the H-wave occurs only during the initial

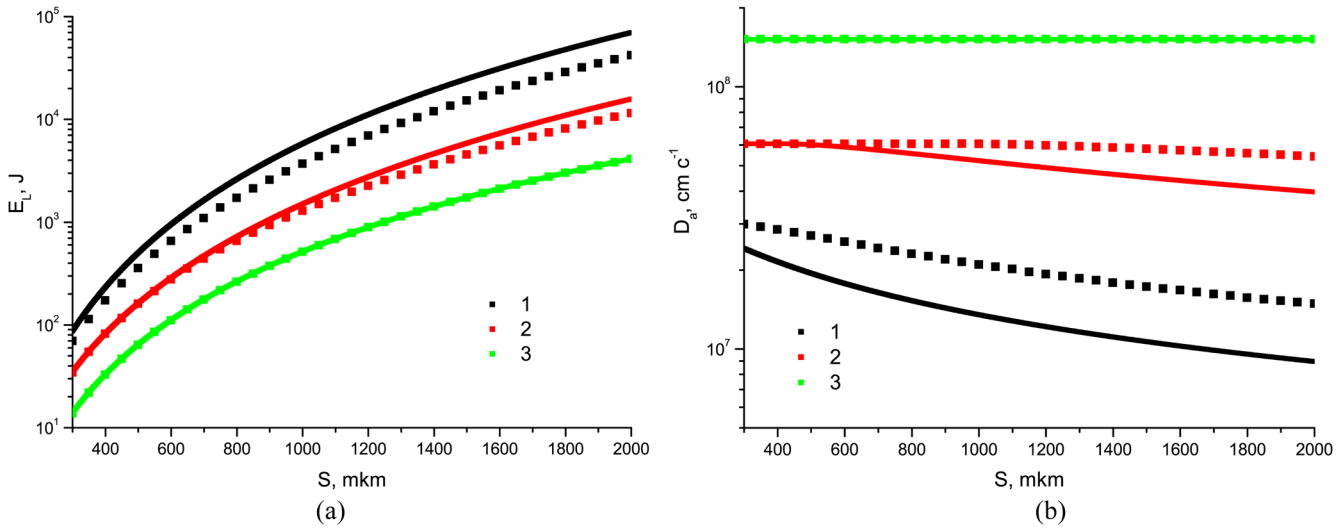

FIG. 5. Dependences of optimal pulse energy (a) and average ionization wave velocity (b) on layer thickness S at a laser intensity of 10^{14} W cm^{-2} for two wavelengths 0.53 μm (solid lines) and 0.35 μm (dotted lines) and for three densities 10 mg cm^{-3} (black lines), 5 mg cm^{-3} (red lines), and 2 mg cm^{-3} (green lines).

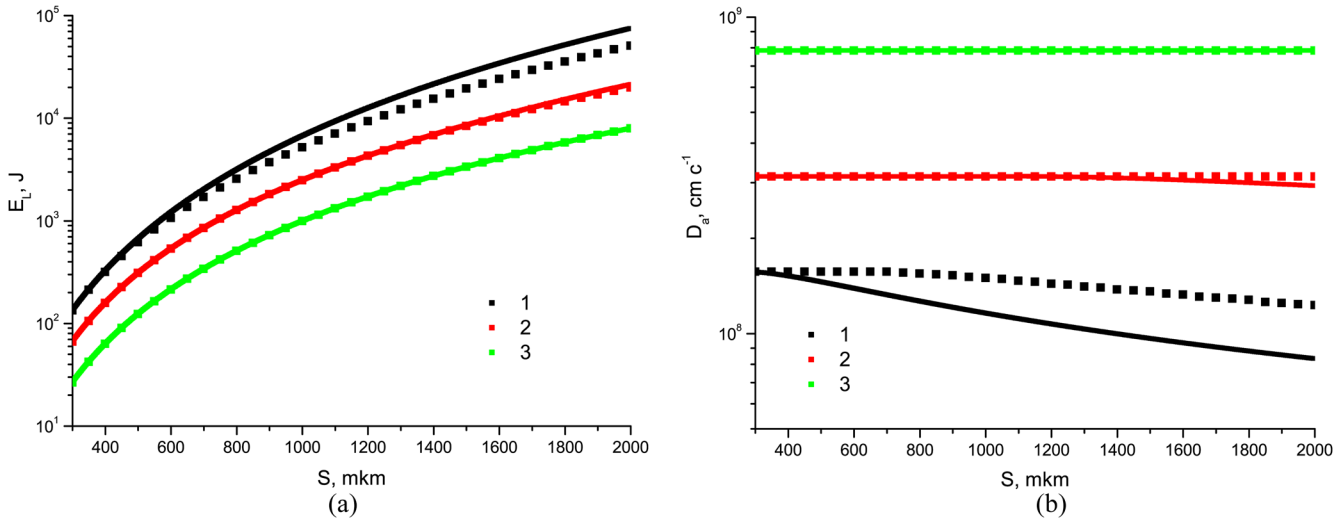

FIG. 6. Dependences of optimal pulse energy (a) and average ionization wave velocity (b) on layer thickness S at a laser intensity of 10^{15} W cm^{-2} for two wavelengths 0.53 μm (solid lines) and 0.35 μm (dotted lines) and for three densities 10 mg cm^{-3} (black lines), 5 mg cm^{-3} (red lines), and 2 mg cm^{-3} (green lines).

stage of wave propagation, and the decrease in the OI-wave velocity is manifested over time.

V. CONCLUSIONS

An analytical solution has been found for the velocity of a non-stationary plane ionization wave supported by a laser pulse of time-constant intensity in a layer of low-Z porous substance of subcritical density. The solution is based on competition between the ordinary ionization wave in a continuous medium and the wave of homogenization of a porous substance. The solution gives the degree of delay of the ionization wave in a layer of porous material compared with an equivalent layer of continuous material as a function of laser intensity and wavelength, layer thickness, average density, and pore size of the porous substance.

2D corrections to the 1D solution have been estimated analytically under the conditions of experiments on laser beam interaction with a porous layer. With such corrections taken into account, the solution is in quantitative agreement with measured velocity of a laser-supported ionization wave in a layer of porous substance in various experiments.

The validation of the 2D model by the available experimental data indicates that the basic approach of the model in using a 1D analytical solution for the velocity of a laser-supported ionization wave is indeed appropriate for achieving the main goal of the paper, namely, scaling of the absorbed laser energy transfer rate in a low-density substance for application to ICF and EOS research.

The parameters of the laser beam (pulse energy and duration, beam radius) that ensure the generation of a plane ionization wave with the predicted velocity in a layer of porous substance of subcritical density are determined in the ranges of laser intensity 10^{14}–10^{15} W cm^{-2} and wavelength 0.35–0.53 μm, which meet the interests of practical applications in inertial confinement fusion and equation of state research. Ionization wave velocity scaling is presented for an optimal laser pulse of duration equal to the time of wave passage through the layer when the laser beam diameter is equal to the porous layer thickness. Fine-pore substances with a pore size of 1 μm and densities from 1 to 10 mg cm^{-3} have been considered. At a given layer thickness, the optimal pulse energy increases with increasing density, laser intensity, and wavelength. For a layer of thickness 1000 μm, there is an increase in pulse energy from 500 J for a pulse with intensity 10^{14} W cm^{-2} and wavelength 0.35 μm at a density ρ = 2 mg cm^{-3} to 6 kJ for a pulse with intensity 10^{15} W cm^{-2} and wavelength 0.53 μm at a density ρ = 10 mg cm^{-3}. The dependences of the average wave velocity and pulse energy for the lowest density of 2 mg cm^{-3} are not distinguished in layers with thicknesses less than 1000 μm for both wavelengths and both laser intensities. The reason is that the ionization wave propagates with the velocity of the homogenization wave, which decelerates the ionization wave at such a low substance density during the entire passage time. At the higher densities of 5 mg cm^{-3} and, especially, 10 mg cm^{-3}, the effect of decreasing wave velocity with increasing layer thickness is manifested. This decrease is stronger at longer laser wavelengths, because at such large densities the deceleration of the ionization wave by the homogenization wave only occurs during the initial stage of wave propagation.

ACKNOWLEDGMENTS

This work was carried out within the framework of the program of the National Center for Physics and Mathematics in the section of High Energy Density Physics.

AUTHOR DECLARATIONS

Conflict of Interest

The authors have no conflicts to disclose.

Author Contributions

S. Yu. Gus'kov: Conceptualization (equal); Data curation (equal); Formal analysis (equal); Investigation (equal); Methodology (equal); Supervision (equal); Validation (equal); Visualization (equal); Writing – original draft (equal). **R. A. Yakhin**: Data curation (equal); Formal analysis (equal); Software (equal); Validation (equal); Visualization (equal); Writing – original draft (equal).

DATA AVAILABILITY

The data that support the findings of this study are available from the corresponding author upon reasonable request.

REFERENCES

[1] S. Yu. Gus'kov and V. B. Rozanov, "Interaction of laser radiation with a porous medium and formation of a nonequilibrium plasma," Quantum Electron. **27**, 696 (1997).
[2] S. Yu. Gus'kov, "Nonequilibrium laser-produced plasma of volume-structured media and inertial-confined-fusion applications," J. Russ. Laser Res. **31**, 574 (2010).
[3] A. E. Bugrov, S. Yu. Gus'kov, V. B. Rozanov, I. N. Burdonskii, V. V. Gavrilov, A. Y. Gol'tsov, E. V. Zhuzhukalo, N. G. Koval'skii, M. I. Pergament, and V. M. Petryakov, "Interaction of a high-power laser beam with low-density porous media," J. Exp. Theor. Phys. **84**, 497 (1997).
[4] A. Caruso, C. Strangio, S. Yu. Gus'kov, and V. B. Rozanov, "Interaction experiments of laser light with low density supercritical foams at the AEEF ABC facility," Laser Part. Beams **18**, 25 (2000).
[5] M. Desselberger, M. Jones, J. Edwards, M. Dunne, and O. Willi, "Use of X-ray preheated foam layers to reduce beam structure imprint in laser-driven targets," Phys. Rev. Lett. **74**, 2961 (1995).
[6] S. Depierreux, C. Labaune, D. T. Michel, C. Stenz, P. Nicolai, M. Grech, G. Riazuelo, S. Weber, C. Riconda, V. T. Tikhonchuk, P. Loiseau, N. G. Borisenko, W. Nazarov, S. Huller, D. Pesme, M. Casanova, J. Limpouch, C. Meyer, P. Di-Nicola, R. Wrobel, E. Alozy, P. Romary, G. Thiell, G. Soullie, C. Reverdin, and B. Villette, "Laser smoothing and imprint reduction with a foam layer in the multikilojoule regime," Phys. Rev. Lett. **102**, 195005 (2009).
[7] T. Hall, D. Batani, W. Nazarov, M. Koenig, and A. Benuzzi, "Recent advances in laser–plasma experiments using foams," Laser Part. Beams **20**, 303 (2002).
[8] M. Cipriani, S. Yu. Gus'kov, F. Consoli, R. De Angelis, A. A. Rupasov, P. Andreoli, G. Cristofari, G. Di Giorgio, and M. Salvadori, "Time-dependent measurement of high-power laser light reflection by low-Z foam plasma," High Power Laser Sci. Eng. **9**, e40 (2021).
[9] K. Nagai, C. S. A. Musgrave, and W. Nazarov, "A review of low density porous materials used in laser plasma experiments," Phys. Plasmas **25**, 030501 (2018).
[10] S. Yu. Gus'kov, N. V. Zmitrenko, and V. B. Rozanov, "The laser greenhouse thermonuclear target with distributed absorption of laser energy," J. Exp. Theor. Phys. **81**, 296 (1995).
[11] M. Dunne, M. Borghesi, A. Iwase, M. W. Jones, R. Taylor, O. Willi, R. Gibson, S. R. Goldman, J. Mack, and R. Watt, Phys. Rev. Lett. **75**, 3858 (1995).
[12] S. Y. Gus'kov and Y. A. Merkul'ev, "Low-density absorber—Converter in direct-irradiation laser thermonuclear targets," Quantum Electron. **31**, 311 (2001).
[13] D. Batani, A. Balducci, W. Nazarov, T. Löwer, T. Hall, M. Koenig, B. Faral, A. Benuzzi, and M. Temporal, "Use of low-density foams as pressure amplifiers in equation-of-state experiments with laser-driven shock waves," Phys. Rev. E **63**, 046410 (2001).
[14] A. Benuzzi, M. Koenig, J. Krishnan, B. Faral, W. Nazarov, M. Temporal, D. Batani, L. Müller, F. Torsiello, T. Hall, and N. Grandjouan, "Dynamics of laser produced shocks in foam–solid targets," Phys. Plasmas **5**, 2827 (1998).
[15] M. Temporal, S. Atzeni, D. Batani, and M. Koenig, "Analysis of the impedance mismatch effect in foam-solid targets compressed by laser-driven shock waves," Eur. Phys. J. D **12**, 509 (2000).
[16] I. A. Belov, S. A. Bel'kov, S. V. Bondarenko, G. A. Vergunova, A. Yu. Voronin, S. G. Garanin, S. Y. Golovkin, S. Y. Gus'kov, N. N. Demchenko, V. N. Derkach *et al.*, "Shock-wave pressure transfer to a solid target with porous absorber of high-power laser pulse," J. Exp. Theor. Phys. **134**(3), 340 (2022).
[17] S. Gus'kov, J. Limpouch, P. Nicolai, and V. Tikhonchuk, "Laser-supported ionization wave in under-dense gases and foams," Phys. Plasmas **18**, 103114 (2011).
[18] J. Denavit and D. W. Phillion, "Laser ionization and heating of gas targets for long-scale-length instability experiments," Phys. Plasmas **1**(6), 1971 (1994).
[19] J. Colvin, H. Matsukuma, K. Brown, J. Davis, G. Kemp, K. Koga, N. Tanaka, A. Yogo, Z. Zhang, H. Nishimura, and K. Fournier, "The effects of microstructure on

propagation of laser-driven radiative heat waves in under-dense high-Z plasma," Phys. Plasmas **25**, 032702 (2018).
[20]M. Cipriani, S. Yu. Gus'kov, R. De Angelis, F. Consoli, A. Rupasov, P. Andreoli, G. Cristofari, and G. Di Giorgio, "Laser-driven hydrothermal wave speed in low-Z foam of overcritical density," Phys. Plasmas **25**, 092704 (2018).
[21]P. Nicolai, M. Olazabal-Loumé, S. Fujioka, A. Sunahara, N. Borisenko, S. Gus'kov, A. Orekov, M. Grech, G. Riazuelo, C. Labaune, J. Velechowski, and V. Tikhonchuk, "Experimental evidence of foam homogenization," Phys. Plasmas **19**, 113105 (2012).
[22]N. G. Borisenko and Y. A. Merkuliev, "Preheating of a target by laser radiation through plasma and polymer aerogel," J. Russ. Laser Res. **31**(3), 256 (2010).
[23]A. M. Khalenkov, N. G. Borisenko, V. N. Kondrashov, Yu.A. Merkuliev, J. Limpouch, and V. G. Pimenov, "Experience of micro-heterogeneous target fabrication to study energy transport in plasma near critical density," Laser Part. Beams **24**, 283–290 (2006).
[24]O. S. Jones, G. E. Kemp, S. H. Langer, B. J. Winjum, R. L. Berger, J. S. Oakdale, M. A. Belyaev, J. Biener, M. M. Biener, D. A. Mariscal, J. L. Milovich, M. Stadermann, P. A. Sterne, and S. C. Wilks, "Experimental and calculational investigation of laser-heated additive manufactured foams," Phys. Plasmas **28**, 022709 (2021).
[25]V. Tikhonchuk, T. Gong, N. Jourdain, O. Renner, F. P. Condamine, K. Q. Pan, W. Nazarov, L. Hudec, J. Limpouch, R. Liska, M. Krůs, F. Wang, D. Yang, S. W. Li, Z. C. Li, Z. Y. Guan, Y. G. Liu, T. Xu, X. S. Peng, X. M. Liu, Y. L. Li, J. Li, T. M. Song, J. M. Yang, S. E. Jiang, B. H. Zhang, W. Y. Huo, G. Ren, Y. H. Chen, W. Zheng, and S. Weber, "Studies of laser-plasma interaction physics with low-density targets for direct-drive inertial confinement fusion on the Shenguang III prototype," Matter Radiat. Extremes **6**, 025902 (2021).
[26]J. Velechovsky, J. Limpouch, R. Liska, and V. Tikhonchuk, "Hydrodynamic modeling of laser interaction with micro-structured targets," Plasma Phys. Control. Fusion **58**, 095004 (2016).
[27]M. Cipriani, S. Gus'kov, R. De Angelis, F. Consoli, A. Rupasov, P. Andreoli, G. Cristofari, G. Di Giorgio, and F. Ingenito, "Laser-supported hydrothermal wave in low-dense porous substance," Laser Part. Beams **36**, 121–128 (2018).
[28]M. Belyaev, R. Berger, O. Jones, S. Langer, and D. Mariscal, "Laser propagation in a subcritical foam: Ion and electron heating," Phys. Plasmas **25**, 123109 (2018).
[29]V. Tikhonchuk, Y. J. Gu, O. Klimo, J. Limpouch, and S. Weber, "Studies of laser-plasma interaction physics with low-density targets for direct-drive inertial confinement schemes," Matter Radiat. Extremes **4**, 045402 (2019).
[30]M. A. Belyaev, R. L. Berger, O. S. Jones, S. H. Langer, D. A. Mariscal, J. Milovich, and B. Winjum, "Laser propagation in a subcritical foam: Subgrid model," Phys. Plasmas **27**, 112710 (2020).
[31]L. Hudec, A. Gintrand, J. Limpouch, R. Liska, S. Shekhanov, V. T. Tikhonchuk, and S. Weber, "Hybrid ablation–expansion model for laser interaction with low-density foams," Phys. Plasmas **30**, 042704 (2023).
[32]S. Yu. Gus'kov, P. A. Kuchugov, and R. A. Yakhin, "Duration and distance of a laser-driven shock wave formation in a plasma with subcritical density," Phys. Plasmas **28**, 092108 (2021).
[33]V. V. Gavrilov, A. Yu. Gol'tsov, N. G. Koval'skii, S. N. Koptyaev, A. I. Magunov, T. A. Pikuz, I. Yu. Skobelev, and A. Ya. Faenov, "X-ray spectral measurement of high-temperature plasma parameters in porous targets irradiated with high-power laser pulses," Quantum Electron. **31**, 1071 (2001).
[34]V. F. Tishkin, V. V. Nikishin, I. V. Popov, and A. P. Favorskii, "Finite difference schemes of three-dimensional gas dynamics for the study of Richtmyer–Meshkov instability," Mat. Model. **7**(5), 15 (1995).
[35]S. A. Bel'kov, S. V. Bondarenko, G. A. Vergunova, S. G. Garanin, S. Yu. Gus'kov, N. N. Demchenko, I. Y. Doskoch, N. V. Zmitrenko, P. A. Kuchugov, V. B. Rozanov, R. V. Stepanov, and R. A. Yakhin, "Effect of spatial nonuniformity of heating on compression and burning of a thermonuclear target under direct multibeam irradiation by a megajoule laser pulse," J. Exp. Theor. Phys. **124**, 341 (2017).
[36]S. Y. Gus'kov, M. Cipriani, R. De Angelis, F. Consoli, A. A. Rupasov, P. Andreoli, G. Cristofari, and G. Di Giorgio, "Absorption coefficient for nanosecond laser pulse in porous material," Plasma Phys. Controlled Fusion **57**, 125004 (2015).